

Interstellar Extinction Law toward the Galactic Center II: V, J, H, and K_S Bands

Shogo Nishiyama¹, Tetsuya Nagata², Motohide Tamura¹, Ryo Kandori¹, Hirofumi Hatano³,
Shuji Sato³, and Koji Sugitani⁴

ABSTRACT

We have determined the ratios of total to selective extinction directly from observations in the optical V band and near-infrared J band toward the Galactic center. The OGLE (Optical Gravitational Lensing Experiment) Galactic bulge fields have been observed with the SIRIUS camera on the IRSF telescope, and we obtain $A_V/E_{V-J} = 1.251 \pm 0.014$ and $A_J/E_{V-J} = 0.225 \pm 0.007$. From these ratios, we have derived $A_J/A_V = 0.188 \pm 0.005$; if we combine A_J/A_V with the near-infrared extinction ratios obtained by Nishiyama et al. for more reddened fields near the Galactic center, we get $A_V : A_J : A_H : A_{K_S} = 1 : 0.188 : 0.108 : 0.062$, which implies steeply declining extinction toward the longer wavelengths. In particular, it is striking that the K_S band extinction is $\approx 1/16$ of the visual extinction A_V , much smaller than one tenth of A_V so far employed.

Subject headings: dust, extinction — stars: horizontal-branch — Galaxy: center

1. INTRODUCTION

The wavelength dependence of interstellar extinction provides important diagnostic information about the dust grain properties. Interstellar extinction law shows a large range of variability from one line of sight to another, especially in the ultraviolet and optical wavelengths. In comparing the wavelength dependence among different lines of sight, the normalization of the extinction curves by the total extinction A_V , instead of the usual color excess E_{B-V} , is vitally important, as Cardelli, Clayton, & Mathis (1989, CCM) have shown. According to CCM, the variation in Galactic extinction curves from the ultraviolet to the optical is described by a single parameter, which itself is the ratio of total to selective extinction

$R_V = A_V/E_{B-V}$. Thus the ratio R_V , or more generally $R_\lambda = A_\lambda/E_{\lambda'-\lambda}$, is very important, although very difficult to obtain. An usual way to determine R_V is to extrapolate the ratio of color excesses $E_{\lambda-V}/E_{B-V}$ to $\lambda = \infty$ with reference to *some model*, and can be compromised by *emission* or *scattering* by dust grains near the stars.

The past decade has seen a new method to determine the ratio of total to selective extinction R_λ . The method was first proposed by Woźniak & Stanek (1996); in essence, it simply measures the regression of the mean color of red clump (RC) stars in the Galactic bulge on their mean magnitude (RC method). The increase in the amount of dust in a line of sight causes the clump fainter and redder. The slope of these changes in a color-magnitude diagram (CMD) is equivalent to R_λ . The method has been developed by Stanek (1996), Udalski (2003), and Sumi (2004) in the V and I bands¹, and recently applied to the near-infrared wavebands by Nishiyama et al. (2006a, hereafter paper I).

¹National Astronomical Observatory of Japan, Mitaka, Tokyo 181-8588, Japan; shogo@optik.mtk.nao.ac.jp

²Department of Astronomy, Kyoto University, Kyoto 606-8502, Japan

³Department of Astrophysics, Nagoya University, Nagoya 464-8602, Japan

⁴Graduate School of Natural Sciences, Nagoya City University, Nagoya 467-8501, Japan

¹They regard their I filter as similar to the Landolt Cousins I , whose effective wavelength is about $0.80\mu\text{m}$.

As a result, a somewhat surprising suggestion was first made by Popowski (2000) for the interstellar extinction toward the Galactic bulge; the ratio of total to selective extinction $R_{VI} = A_V/E_{V-I}$ is approximately 2.0, much smaller than the ratio 2.5 for the standard ($R_V = 3.1$) CCM extinction curve (Udalski 2003). This was confirmed by Sumi (2004) in a larger number of fields. Thus the V ($0.55\mu\text{m}$) to I ($0.80\mu\text{m}$) part of the extinction curve toward the Galactic bulge seems to be characterized by a smaller R_{VI} . In the near infrared, the extinction law is frequently referred to as “universal”, and in fact CCM gives an R_V -independent curve. However, paper I have shown that the near-infrared extinction curve toward the Galactic Center (GC) is different from those in the literature, having also smaller A_H/E_{J-H} and A_{K_S}/E_{H-K_S} .

In this paper, we apply the RC method and extend the R_λ determination to the J band ($1.25\mu\text{m}$) by measuring the J magnitude of the stars whose V photometry was obtained in Udalski (2003). Furthermore, assuming that the extinction curve can be extended to more heavily reddened regions observed in paper I, we estimate A_λ/A_V at J , H , and K_S wavelengths.

2. Observation, Data Reduction, and Analysis

2.1. Near-infrared Observations

All observations in the near-infrared wavelengths were made with the SIRIUS camera (Simultaneous InfraRed Imager for Unbiased Survey; Nagashima et al. 1999; Nagayama et al. 2002) attached to the 1.4 m telescope IRSF (InfraRed Survey Facility), on the nights of 2004 May 18 and 19. The SIRIUS camera provides photometric images of a $7'7 \times 7'7$ area of sky in three near-infrared wavebands J ($1.25\mu\text{m}$), H ($1.63\mu\text{m}$), and K_S ($2.14\mu\text{m}$) simultaneously. The detectors are three 1024×1024 HgCdTe arrays, with a scale of $0''.45 \text{ pixel}^{-1}$. The IRSF/SIRIUS system is similar to the MKO system (Tokunaga et al. 2002).

Over the range of $17^{\text{h}}52^{\text{m}} \lesssim \text{R.A. (J2000.0)} \lesssim 17^{\text{h}}56^{\text{m}}$ and $-30^{\circ}2 \lesssim \text{Dec. (J2000.0)} \lesssim -29^{\circ}5$, 32 images in each band were obtained (Fig. 1). These fields correspond to the region “A” ($l \approx 0^\circ, b \approx -2^\circ$) of Udalski (2003) in the Optical Gravitational Lensing Experiment (OGLE) II maps of the

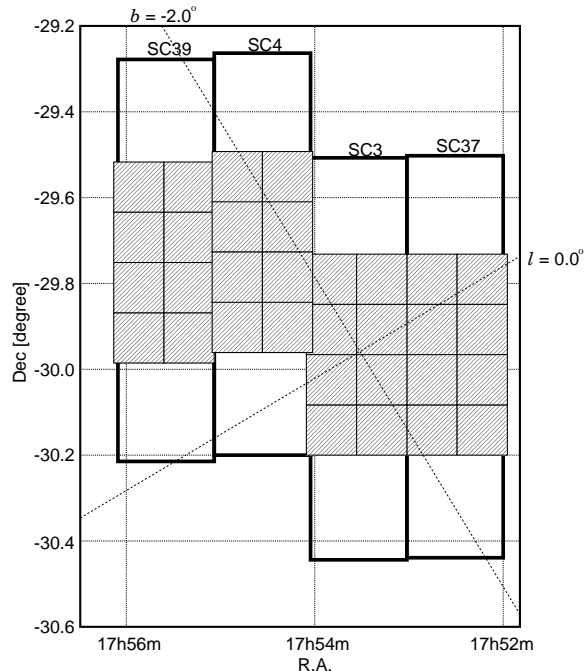


Fig. 1.— Observed area and fields used for data analysis. Thick-line rectangles, labeled as “SC39”, “SC4”, “SC3”, and “SC37” show the areas observed by the OGLE project. The fields observed by IRSF/SIRIUS are shown by hatched squares.

Galactic bulge in the V and I bands² with an absolute photometric accuracy of 0.01-0.02 mag (Udalski et al. 2002). The data files containing the photometry were downloaded from the OGLE website³. The Udalski (2003) “A” region consists of the five fields SC3, SC4, SC5, SC37, and SC39 (Fig. 1), but the SC5 data were excluded from the following analysis because it suffers from the heaviest extinction and its V magnitudes become unreliable, as Udalski (2003) also pointed out.

The observing weather was photometric, with seeing of $\sim 1''.1$ in the J band. Flat fields were obtained during each clear evening and morning twilight. Dark frames were taken at the end of each observing night. A single image comprises 10

²In this paper, we do not use the I band data, because the OGLE I band filter has a wider long-wavelength wing of transmission contrary to the sharper drop of the standard I band filter, and the relation between V and I extinction has been already studied by Udalski (2003), and Sumi (2004).

³http://bulge.princeton.edu/~ogle/ogle2/bulge_maps.html

dithered 5 sec exposures.

The SIRIUS camera provides three (J , H , and K_S) images simultaneously, and thus we have the data sets of the same region in the three bands. However, the uncertainties in the H and K_S photometry are larger, and the range of extinction is smaller, about a half (H) and a third (K_S) of that in the J band⁴. Therefore we have obtained reliable results only in the J band.

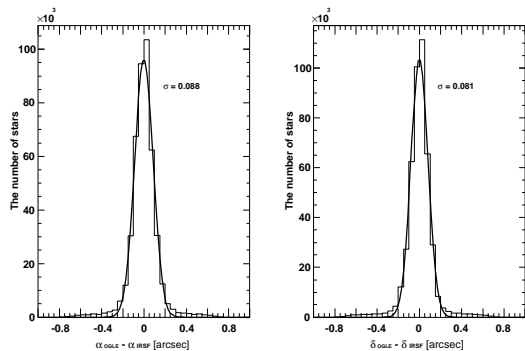


Fig. 2.— Histograms of the positional difference between the OGLE and IRSF coordinates for cross-identified stars in R.A. (*left*) and Dec. (*right*). The values of σ obtained by fitting with a Gauss function are $0''.088$ in R.A. and $0''.081$ in Dec., respectively. The positional offsets between the OGLE and IRSF coordinates were already corrected.

IRAF (Image Reduction and Analysis Facility)⁵ software package was used to perform dark and flat-field corrections, followed by sky background estimation and subtraction. Photometry, including point spread function (PSF) fitting, was carried out with the DAOPHOT package (Stetson 1987). We used the DAOFIND task to identify

⁴In paper I, we have observed fields closer to the GC where the range of extinction is large (about 3.5 mag in the J band), and thus we were able to determine the extinction ratio in the J , H , and K_S bands accurately. However, the fields observed in this study are located at $b \sim -2^\circ$, and the range of extinction is 0.5 mag in the J band (see the bottom panel in Fig. 4), which is less than 0.2 mag in the K_S band.

⁵IRAF is distributed by the National Optical Astronomy Observatory, which is operated by the Association of Universities for Research in Astronomy, Inc., under cooperative agreement with the National Science Foundation.

point sources, and the sources were then input for PSF-fitting photometry to the ALLSTAR task. About 20 sources were used to construct the PSF for each image.

Each image was calibrated with the standard star #9172 (Persson et al. 1998), which was observed every half an hour. We assumed that #9172 is $J = 12.48$ in the IRSF/SIRIUS system. The average of the zero point uncertainties and the 10σ limiting magnitude in the J band were ~ 0.02 mag and 16.8 mag, respectively.

Astrometric calibration was performed, field by field, with reference to the positions of stars in the 2MASS point source catalog (Skrutskie et al. 2006). Only the stars with the photometric error of less than 0.05 mag in the 2MASS and our catalog were used for the calibration. The positional difference was finally calculated by using the stars of $\lesssim 0.1$ mag photometric error, and we obtained the standard deviation of the positional difference better than $0''.1$.

2.2. Cross-identification of the SIRIUS and the OGLE source

The stars found with IRSF/SIRIUS and OGLE have been cross-identified, field by field, using a simple positional correlation. The procedure consists of two steps. First, identification was performed with large radius ($1''.5$) to evaluate astrometric offset between IRSF and OGLE coordinates. We found that the offsets in R.A. and Dec. are in the range from $-0''.7$ to $+0''.1$, and from $+0''.1$ to $+0''.4$, respectively. The offsets seem to depend on the position in the OGLE field. Second, the OGLE coordinates were corrected for these offsets, and a search radius of $0''.7$ was used for the identification.

We show the histograms of positional differences of the finally identified stars in Fig. 2. We found $\sim 25,000$ matches in each field with an rms error in the difference between SIRIUS and OGLE coordinates $0''.13$ in R.A. and Dec. The values of σ obtained by fitting with a Gauss function are $0''.088$ in R.A. and $0''.081$ in Dec.

2.3. Data Analysis

To measure the ratios of total to selective extinction A_V/E_{V-J} and A_J/E_{V-J} , we selected the bulge RC stars, which constitute a compact and

well-defined clump in a CMD, and are thus good tracers of extinction and reddening. The V versus $V - J$ CMD constructed with the IRSF and OGLE data is shown in Fig. 3. In this analysis we follow the procedure described in Udalski (2003), Sumi (2004), and paper I.

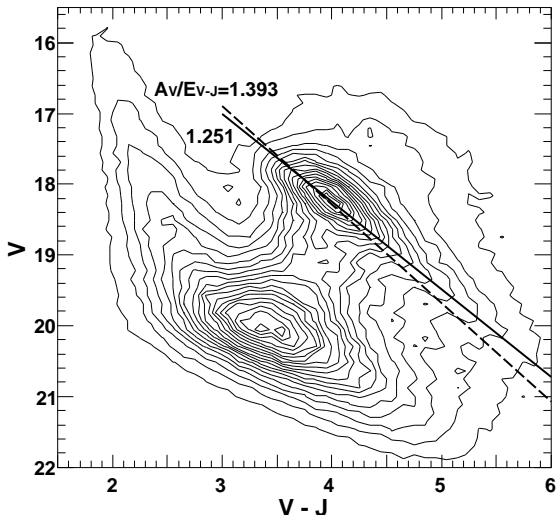


Fig. 3.— V versus $V - J$ color magnitude diagram of the OGLE bulge fields. Contours are from 0 to 1600, linearly spaced by 80. The *solid* and *dashed* lines show the direction of the interstellar extinction with $A_V/E_{V-J} = 1.251$ (this work), and 1.393 (Cardelli, Clayton, & Mathis 1989, $R_V = 3.1$), respectively.

First, we divide each field of SIRIUS into nine subfields of $\sim 2'.8 \times 2'.8$ on the sky. Then we construct V versus $V - J$ and J versus $V - J$ CMDs for each subfield. Second, in the CMDs, we extract stars in the region dominated by RC stars, and the stars are used to make magnitude histograms (luminosity function, see also Fig.2 in paper I). The peaks of RC stars are fitted with a Gaussian function. Third, the stars in the range fitted above are employed to see the distribution of RC stars in the color $V - J$, and the color peaks of RC stars are also fitted with a Gaussian function. Since the mean V magnitudes of RC stars become too faint in highly reddened fields, estimates of the peak magnitudes and the colors of RC stars can be unreliable in such fields. To avoid this problem, we do not use the subfields in which we could not

find a clear peak of RC stars. Note that this exclusion was made in the second and third steps, so a field employed in the J versus $V - J$ CMD can be excluded in the V versus $V - J$ CMD if its V distribution does not have a clear Gaussian peak, and vice versa. As a result, 48 (V versus $V - J$) and 8 (J versus $V - J$) out of 288 (32×9) subfields were excluded from our analysis. Therefore the data points of the two CMD are not identical, and the resultant slopes do not necessarily satisfy the relation $A_V/E_{V-J} = A_J/E_{V-J} + 1^6$.

3. Results

Combining the IRSF J band and the OGLE V band data sets, we have made the V versus $V - J$ (*top panel* in Fig. 4), and J versus $V - J$ (*bottom panel*) CMDs in which the location of the RC magnitude and color *peaks* are shown. Error bars include uncertainties in the RC peak and photometric calibration. The least-squares fits to the data points provide us with the slope in the CMDs, $A_V/E_{V-J} = 1.255 \pm 0.004$ and $A_J/E_{V-J} = 0.225 \pm 0.005$.

The errors in the slopes obtained by using the least-squares fit seem to be underestimated because the dispersion of the data points is large compared with the error bars, which is particularly noticeable in the J versus $V - J$ CMD. Hence we estimated the errors of the slopes by fixing the χ^2 of the fit to equal the number of degrees of freedom, $\chi^2/\text{dof} = 1$, under the assumption that the errors are all equal. Application of this procedure to the data in both CMDs results in $A_V/E_{V-J} = 1.251 \pm 0.014$ and $A_J/E_{V-J} = 0.225 \pm 0.007$.

These ratios of total to selective extinction provide the ratio of total extinction A_J/A_V , with a simple algebra of $((A_V/E_{V-J}) - 1)/(A_V/E_{V-J})$ and $(A_J/E_{V-J})/((A_J/E_{V-J})+1)$, yielding $A_J/A_V = 0.201 \pm 0.011$ (from A_V/E_{V-J}) and $A_J/A_V = 0.184 \pm 0.006$ (from A_J/E_{V-J}). Therefore we obtain the weighted mean and error of them, $A_J/A_V = 0.188 \pm 0.005$. However, the difference of the two values is 0.017, and the combined sigma is $\sqrt{0.011^2 + 0.006^2} = 0.013$. Hence A_J/A_V could have an error of an order of 0.01.

⁶We made a J versus $V - J$ CMD excluding 48 subfields, which are not used in V versus $V - J$, and confirmed that the exclusion of them changes the slope in the CMD by only 0.002.

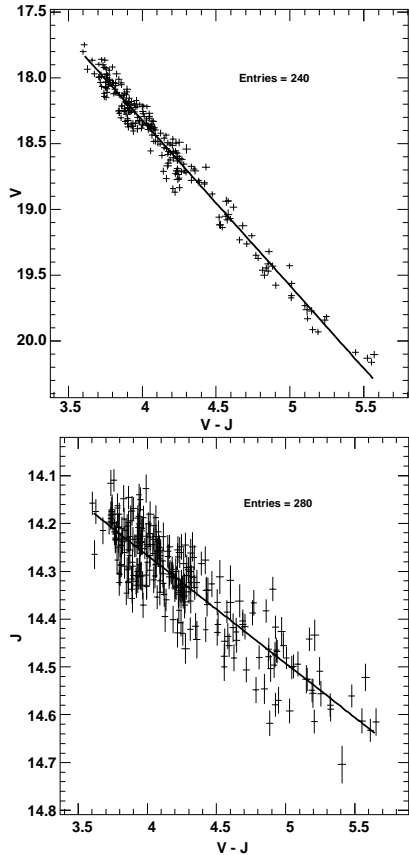


Fig. 4.— Location of RC peaks in V versus $V - J$ (*top*) and J versus $V - J$ (*bottom*) CMDs. The solid lines are the least-squares fits to the data points.

4. Discussion

4.1. Reliability of Our Data Sets

The faintest data points in the CMDs (Fig. 4) are $V = 20.2$ and $J = 14.7$. Udalski (2003) set a safety margin and regarded his points as complete to the limit of $V = 20.7$, which is still fainter than our faintest data point by 0.5 mag. As described in section 2, the limiting magnitude in the J band is 16.8, also much fainter than $J = 14.7$. Therefore these margins seem to be large enough to have the mean magnitude of RC stars reliably measured.

The peak magnitude of RC stars could be altered by the dropping completeness. Therefore we have checked the completeness and the change of the peak magnitudes. First, we have made exper-

iments in which we added artificial stars of various known magnitudes to our original images, and subjected them to the same procedure described in §2.1. The detection rates drop as the magnitude becomes fainter; $\approx 95\%$ at $J = 14$, $\approx 85\%$ at $J = 15$, $\approx 70\%$ at $J = 16$. Second, we have reconstructed luminosity functions with the detection rates compensated, and fitted the RC peaks again. Comparing the RC peak magnitudes with reconstructed ones, we have obtained that the mean difference between them is 0.017 mag, and its rms is 0.006. The rms is very small compared to the error of each data points in the CMDs, typically 0.02-0.03 mag. We cannot find clear dependence of the difference on the peak magnitude, and on the number of stars. Hence we can conclude that the completeness effect does not change the slopes in the CMDs.

The zero-point uncertainty should be checked to derive the slope in CMDs reliably. We examined the internal consistency of the duplicate sources in overlapping regions of adjacent fields. Histograms of mean magnitude difference with the sources of photometric error less than 0.05 mag for each field set are shown by the left panel in Fig. 5. The differences of adjacent fields in the direction of R.A. and Dec. are shown by white and hatched histograms, respectively. We determined the rms of the magnitude difference to be less than 0.02 mag. For another check, we have made comparisons with the 2MASS catalog in the J band. The histogram of the mean difference between the 2MASS and IRSF J magnitudes for each field is shown by the right panel in Fig. 5. The mean and rms variance of the histogram are 0.009 mag and 0.015 mag, respectively. The rms variance is similar to the zero-point uncertainty we derived from the observation of the standard stars. We therefore conclude that the systematic error in our data sets is about 0.02 mag. Note that, in this study, a systematic error does not come from *absolute* zero-point uncertainty, but from *relative* one. Even if the absolute magnitudes of RC stars has a systematic offset, the resultant plots shown in Fig. 4 move as a whole with the slope unchanged. Also, the right panel in Fig. 5 shows that the absolute magnitude offset in the J band is small.

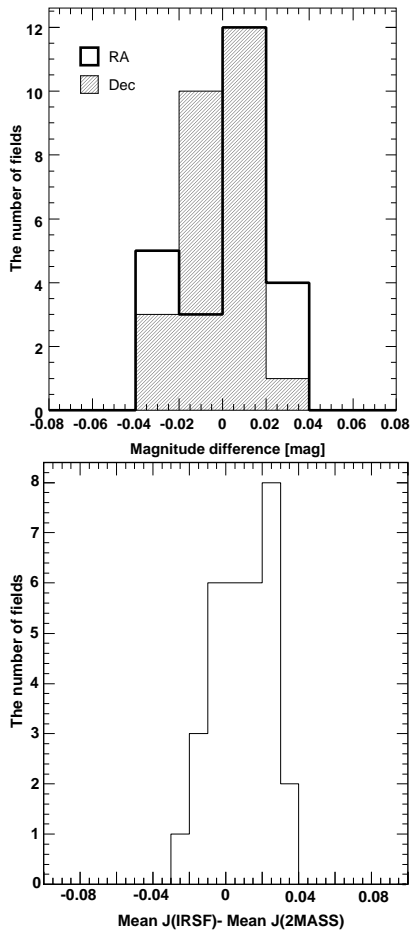


Fig. 5.— (*Top*) Histograms of mean magnitude differences of adjacent fields with the sources of photometric error less than 0.05 mag. The differences in the direction of R.A. and Dec. are shown by *white* and *hatched* histograms, respectively. The mean difference and rms of the histograms are -0.002 and 0.016 (R.A.), and 0.002 and 0.019 (Dec). (*Bottom*) Histogram of mean magnitude difference between 2MASS and IRSF sources in the J band. The mean and rms are 0.009 and 0.015, respectively.

4.2. Error Estimates of R_λ

The difference of distance to RC stars in the observed area could be a factor of the systematic error, which become large in the situation that the distance is correlated with interstellar extinction. However, the distance changes along the Galactic longitude due to the presence of the bar structure (e.g., Nakada et al. 1991), and the extinction seems to change along the Galactic latitude in our observed area (Sumi 2004), suggesting uncorrelation between them. The extent of the observed area in the Galactic longitude is only $1^\circ 1'$, which leads to an only ~ 0.03 mag difference in the brightness of RC stars (Nishiyama et al. 2005), also suggesting the small systematic error by the difference of the distance.

Although population effect of the RC stars is a source of the systematic error, the dependence of the RC brightness on the metallicity is very weak, and the metallicity gradient is expected to be very small in our small observed area (Udalski et al. 2002; Nishiyama et al. 2005). In addition, the metallicity should be again correlated with the interstellar extinction, and this situation seems to be unlikely.

To examine the systematic errors for the population effect and the different distance of RC stars, we made linear fits to the data points in the J versus $V - J$ CMD for four OGLE fields separately, keeping the same slope (0.225) but changing the intersect. The intersects we obtained are 13.37, 13.37, 13.35, and 13.38 for SC37, 3, SC4, and SC39, respectively. Next, to check the dependence of the intersect's deviation on the slope value, we also made linear fits for the four fields, with changing the slope values between 0.211 ($0.255 - 2\sigma$) and 0.239 ($0.255 + 2\sigma$). We could not find any systematic trend, and they are within the error of the intersect, 13.37 ± 0.03 for all subfields. We thus conclude that the difference of the distance and population effect do not affect our results.

The change of the effective wavelength in the J band is very small. As shown in the bottom panel of Fig. 4, the peak magnitudes of RC stars are distributed between $m_J = 14.1$ and 14.7. Using the distance modulus of 14.38 toward the GC (Nishiyama et al. 2006b) and the absolute magnitude $M_J \approx -0.3$ of RC stars (Bonatto et al. 2004), A_J can be estimated to be $0.02 \lesssim A_J \lesssim 0.68$. In

this range of extinction, the effective wavelength in the J band for typical bulge RC stars changes by only $0.002\mu\text{m}$ (see Nishiyama et al. 2006b, §5.1, for more details), and the change of effective wavelength is thus negligible.

4.3. Extinction A_λ/A_V toward Galactic Bulge

In the wavelength range $0.5 - 0.9\mu\text{m}$, extinction toward the Galactic bulge has been characterized by a “steep” curve whose ratio of total to selective extinction is small. The steep extinction curve was introduced to explain the anomalous $(V - I)_0$ color of RC stars in Baade’s window (e.g., Popowski 2000; Gould et al. 2001). The lower value of the ratio of total to selective extinction was also reported from the MACHO V and R photometry ($A_V/E_{V-R} \sim 3.5$, Popowski et al. 2003), and from the OGLE V and I photometry ($R_{VI} = A_V/E_{V-I} \sim 2.0$, Udalski 2003; Sumi 2004) toward the Galactic Bulge. The empirical analytic formula of CCM or Fitzpatrick (1999) corresponding to the extinction toward the Galactic bulge has the single parameter R_V of ≈ 2 , which is much lower than the average value 3.1 for diffuse regions in the local interstellar medium.

The CCM formula uses a simple power law $\lambda^{-1.61}$ in the wavelength region $> 0.9\mu\text{m}$ and it seems independent of R_V . However, since A_V depends on R_V , the ratios A_V/E_{V-J} and A_J/E_{V-J} are dependent on R_V , and these ratios derived in our work⁷ correspond to $R_V \sim 1.8$, which is also very small. The reddening vectors in the V versus $V - J$ CMD for the case of $R_V = 3.1$ and our results are plotted in Fig. 3. The figure shows a clear difference in the reddening direction.

Small values of R_V are generally considered to indicate the prevalence of small dust grains which affect the extinction curve in the ultraviolet - optical wavelengths. Although a substantial number of lines of sight with low R_V values are found especially at high Galactic latitude (e.g., Larson et al. 1996; Larson & Whittet 2005), only a few lines of sight exist with $R_V < 2.0$ (Szomoru & Guhathakurta 1999; Larson & Whittet 2005).

Next, we try to extend the extinction curve to $2\mu\text{m}$. Paper I determined the dependence of

the interstellar extinction in the J , H , and K_S bands toward the GC, and thus we can combine it with the result obtained in this paper to determine A_λ/A_V in the H , and K_S bands. Here we should take into account the variation of the extinction law in different lines of sight, because the area observed in paper I ($|l| \lesssim 2^\circ$ and $0^\circ 5' \lesssim |b| \lesssim 1^\circ 0'$) does not overlap with that of this study. The variation of A_{K_S}/E_{H-K_S} was estimated to be as large as $\sim 7\%$ in the region of $4^\circ \times 2^\circ$ at the GC (paper I), and hence we adopt this value as a variation of A_J/A_V , resulting $A_J/A_V = 0.188 \pm 0.014$ where $0.014 = \sqrt{(0.005)^2 + (0.188 \times 0.07)^2}$. By using the ratio $A_J : A_H : A_{K_S} = 1 : 0.573 \pm 0.009 : 0.331 \pm 0.004$ (paper I), we obtain $A_J/A_V : A_H/A_V : A_{K_S}/A_V = 0.188 \pm 0.014 : 0.108 \pm 0.008 : 0.062 \pm 0.005$.

Table 1: The wavelength dependence of the interstellar extinction.

	IRSF	vdH ⁽¹⁾	CCM ⁽²⁾
A_V/E_{V-J}	1.251 ± 0.014	1.325	1.393
A_J/E_{V-J}	0.225 ± 0.007	0.325	0.393
A_J/A_V	$0.188 \pm 0.014^{(3)}$	0.245	0.282
A_H/A_V	$0.108 \pm 0.008^{(3)}$	0.142	0.190
A_{K_S}/A_V	$0.062 \pm 0.005^{(3)}$	0.088	0.118

References. — (1) van de Hulst (1946); (2) Cardelli, Clayton, & Mathis (1989) for the case of $R_V = 3.1$. (3) The error coming from variation of extinction law in different lines of sight is included.

The resultant A_λ/A_V in the JHK_S wavelength range is a steeply declining function. As shown in Table 1, the CCM curve (for $R_V = 3.1$), which is based on Rieke & Lebofsky (1985), decreases much more slowly toward the longer wavelengths. In particular, the K_S band extinction is slightly greater than one tenth of the visual extinction A_V in the CCM curve, which contrasts with the van de Hulst (1946) curve, where A_{K_S} is slightly less than one tenth of A_V . The derived extinction toward the Galactic bulge decreases more steeply as the wavelength increases. The steep decrease is rather striking, but it was already evident in Messineo et al. (2005) and paper I, where a steep extinction power law index $\alpha \approx 2.0$, consistent with the po-

⁷ $R_V \sim 1.8$ was obtained to reproduce our result $A_J/A_V = 0.193$ by using the CCM formula.

larization law up to $\sim 2.5\mu\text{m}$ (Nagata et al. 1994), was proposed for the GC extinction. To confirm this, deep optical and infrared observations in the V to K_S bands for the same fields with appropriate extinction would be important.

We thank the staff at the South African Astronomical Observatory (SAAO) for their support during our observations. The IRSF/SIRIUS project was initiated and supported by Nagoya University, the National Astronomical Observatory of Japan in collaboration with the SAAO. This work was supported by KAKENHI, Grant-in-Aid for Young Scientists (B) 19740111, and in part by the Grants-in-Aid for the 21st Century COE “The Origin of the Universe and Matter: Physical Elucidation of the Cosmic History” from the MEXT of Japan. This publication makes use of data products from the Two Micron All Sky Survey, which is a joint project of the University of Massachusetts and the Infrared Processing and Aeronautics and Space Administration and the National Science Foundation.

REFERENCES

- Bonatto, C., Bica, E., & Girardi, L. 2004, *A&A*, 415, 571
- Cardelli, J. A., Clayton, G. C., & Mathis, J. S. 1989, *ApJ*, 345, 245 (CCM)
- Dutra, C. M., Santiago, B. X., Bica, E. L. D., & Barbuy, B. 2003, *MNRAS*, 338, 253
- Fitzpatrick, E. L. 1999 *PASP*, 111, 63
- Gould, A., Stutz, A., & Frogel, J. A. 2001, *ApJ*, 547, 590
- Larson, K. A., Whittet, D. C. B., & Hough, J. H. 1996, *ApJ*, 472, 755
- Larson, K. A., & Whittet, D. C. B. 2005, *ApJ*, 623, 897
- Messineo, M., Habing, H. J., Menten, K. M., Omont, A., Sjouwerman, L. O., & Bertoldi, F. 2005, *A&A*, 435, 575
- Nagashima, C., et al. 1999, in *Star Formation 1999*, ed. T. Nakamoto (Nobeyama : Nobeyama Radio Obs.), 397
- Nagata, T., Kobayashi, N., & Sato, S. 1994, *ApJ*, 423, L113
- Nagayama, T., et al. 2003, *Proc. SPIE*, 4841, 459
- Nakada, Y., Deguchi, S., Hashimoto, O., Izumiura, H., Onaka, T., Sekiguchi, K. & Yamamura, I. 1991, *Nature*, 353, 140
- Nishiyama, S., et al. 2005, *ApJ*, 621, L105
- Nishiyama, S., et al. 2006a, *ApJ*, 638, 839 (paper I)
- Nishiyama, S., et al. 2006b, *ApJ*, 647, 1093
- Persson, S. E., Murphy, D. C., Krzeminski, W., Roth, M., & Rieke, M. J. 1998, *AJ*, 116, 2475
- Popowski, P. 2000, *ApJ*, 528, L9
- Popowski, P., Cook, K. H., & Becker, A. C. 2003, *AJ*, 126, 2910
- Rieke, G. H., & Lebofsky, M. J. 1985, *ApJ*, 288, 618
- Skrutskie, M. F., et al. 2006, *AJ*, 131, 1163
- Stanek, K. Z. 1996, *ApJ*, 460, L37
- Stetson, P. B. 1987, *PASP*, 99, 191
- Sumi, T. 2004, *MNRAS*, 349, 193
- Szomoru, A., & Guhathakurta, P. 1999, *AJ*, 117, 2226
- Tokunaga, A. T., Simons, D. A., & Vacca, W. D. 2002, *PASP*, 114, 180
- Udalski, A., et al. 2002, *Acta Astron.*, 52, 217
- Udalski, A. 2003, *ApJ*, 590, 284
- van de Hulst, H. C. 1946, *Rech. Astron. Obs. Utrecht*, 11, 1
- Woźniak, P. R., & Stanek, K. Z. 1996, *ApJ*, 464, 233